

CHARACTERIZATION OF FLUIDS AND POROUS MEDIA TO STUDY FLOW PROCESS

Euclides J. Bonet

DEP-FEM-UNICAMP: P. O. Box 6122, Campinas - SP, 13083-970
bonet@dep.fem.unicamp.br

Rogério F. Martini

DEP-FEM-UNICAMP: P. O. Box 6122, Campinas - SP, 13083-970
rogeriom@dep.fem.unicamp.br

Denis J. Schiozer

DEP-FEM-UNICAMP: P. O. Box 6122, Campinas - SP, 13083-970
denis@dep.fem.unicamp.br

Abstract. Usually heavy oil reservoirs are exploited by heat addition in order to reduce oil viscosity and improve field performance. However, this is not an alternative for offshore reservoirs, especially in the Brazilian case, where many fields are found in deep and ultra-deep waters. The best available recovery method for such fields is water injection, which presents significant differences to the behavior observed for light oil reservoirs due to the characteristics of heavy oils. The objective of this work is to characterize the fluids and a porous media, which will be used to study water injection in a porous rectangular plate with horizontal well, containing viscous oil. Petrophysical characteristics for the rock were determined, namely the porosity, absolute permeability and water oil capillary pressure. An X-ray scanning system permitted the 2D mapping of the rock porosity and permeability. The most pertinent fluid properties measured with traditional methods are reported and pictures of the rock encapsulation process are also presented. Since an unstable displacement is expected due to the high oil viscosity, the water oil relative permeability was obtained for a stable and an unstable viscous oil displacement by water. A tracer test was performed, demonstrating that the rock has satisfactory flow characteristics and also, after calculating the Peclet number and linear dispersion coefficient, equivalent results were obtained with analytical, numerical and experimental methods.

Keywords: Heavy oil, characterization, water injection, tracer, petrophysical properties

1. Introduction

With the more frequent use of horizontal wells and new offshore oil discoveries of viscous oil it is very important to correctly describe the behavior of viscous oil displacement (Santos *et al.*, 1997) in porous media. This work aimed to develop a systematic procedure to assist in the study of such behavior; the methodology adopted involved the characterization of a porous media and a study of the flow process through such a rock when horizontal wells are used both for production and injection; the following petrophysical properties are described: absolute permeability, porosity, relative permeability for oil and water and the corresponding capillary pressure. The x-ray scanning technique employed permitted the generation of a porosity map in two dimensions. With a porosity/permeability correlation it was also possible to display a permeability map.

Regarding the fluid, its kinematic viscosity and density were measured, whereas the flow behavior was inferred through a tracer test. Data gathered from experiments can be used in further stages to assist with the development of simulation models, which are very important during the whole production cycle of oil reservoirs. However, the transformation from laboratory units to field scale units is not straightforward. An initial step in this direction is the use of analytical correlations and/or numerical simulation in the laboratory scale to reproduce the experimental behavior.

2. Characterization of the porous media

2.1. Preparation of the porous media

The porous media is an Eolian sandstone from Botucatu formation obtained from an outcrop in Ribeirão Claro, PR, Brazil. Its petrophysical and petrographic characteristics were described by Gomes *et al.* (1996). It was preliminarily cut in a parallelepiped form (0.88m x 0.33m x 0.032m), as shown in Fig. 1, and a groove was cut in the opposite faces, to operate as horizontal wells, as displayed in Fig. 2.

Figure 3 shows the porous rock inside the encapsulating form and in Fig. 4 one can see the encapsulated porous media connected to the laboratory equipment where the absolute air permeability was measured. At this stage, the porous media had already its external faces covered with an epoxy resin to become impermeable. Figure 4 also shows the flowing terminals that were used as injection points (taps) to guarantee uniform saturation of the porous rock. After

the plate was completely filled with oil, the production phase began; in this phase, only the flowing points (taps) located in the extremes of the plate worked, which is equivalent to horizontal wells producing only by their heels.



Figure 1. Rock place (porous media)



Figure 2. Groove operating as horizontal well



Figure 3. Plate in encapsulating vessel



Figure 4. Encapsulated rock plate and laboratory apparatus

2.2. Petrophysical Tests

Four contiguous samples from the plate were cut and analyzed, as indicated in Fig. 5. The porosity and permeability ranges measured can be seen in Tab. 1.

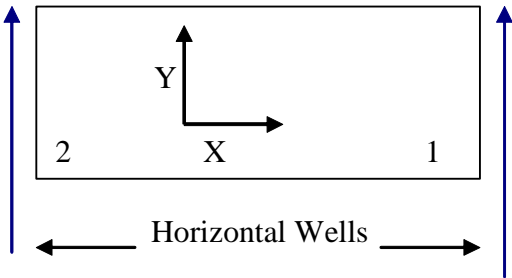


Figure 5. Samples from rock plate

Table 1. Measured values for samples of the porous media.

Sample Property	Measured values	Sample Property	Measured values
Porosity (%) X1 e Y1	20.4-19.9	Permeability (mD) X1 e Y1	478-441
Porosity (%) X2 e Y2	23.1-23.5	Permeability (mD) X2 e Y2	558-502

The plate is a 0.883cm x 0.328cm x 0.032cm parallelepiped with a total volume of $9.268 \times 10^{-3} \text{ m}^3$ and weighing 19.224kg. A Boyle porosimeter and a nitrogen permeameter (Amyx *et al.*, 1960) were used and the results for the entire plate were: pore volume of $2.047 \times 10^{-3} \text{ m}^3$ and absolute permeability of 536mD. The heterogeneity index of Dykstra-Parsons or Koval indicated the sample is greatly homogeneous.

The oil/water relative permeability (Honarpour *et al.*, 2000; Johnson *et al.*, 1959; Jones. and Roszelle, 1978; Marle, 1981) for this rock was obtained from an extensive project. The residual oil saturation (S_{or}) was found to be 24% of the pore volume. The final water relative permeability (K_{rw}) at residual oil saturation varied with the absolute permeability, but for this plate it was 8.0% of the absolute permeability. With the measured values of irreducible water saturation (S_{wi}) and the corresponding oil/water relative permeability (K_{ro}) it is possible to calculate the normalized water saturation, as indicated in Eq. (1). Figure 6 shows the curves for stable displacement; the values are expressed in dimensionless saturation and the base for the relative permeability is the oil effective permeability at initial water saturation. The water oil relative permeability for unstable water/oil displacement (Chuoke *et al.*, 1959; Gomes, 1997) is presented in Fig. 7. Straight lines are typical of unstable displacement; this can be observed in the K_{rw} curve of Fig. 7, which is nearly straight for a great part of the saturation range, before the abrupt rise near the end.

$$S_w^* = \frac{S_w - S_{wi}}{1 - S_{wi} - S_{or}} \quad (1)$$

where S_w^* is the normalized water saturation and S_w is the water saturation.

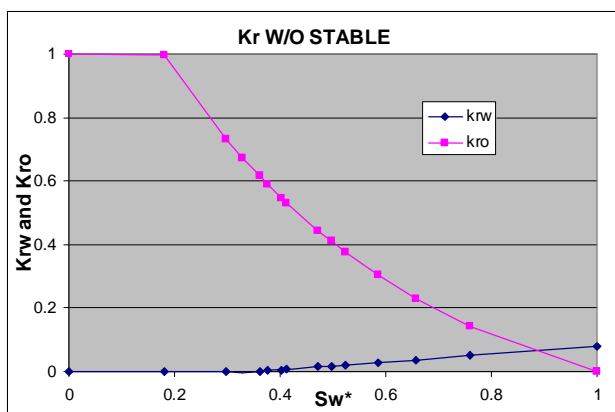


Figure 6. Stable water oil relative permeability

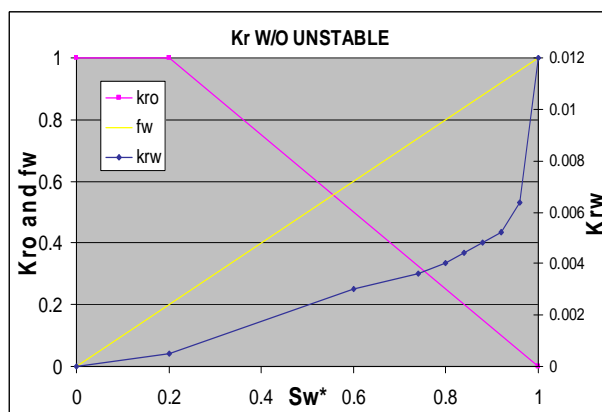


Figure 7. Unstable water oil relative permeability

The oil/water capillary pressure was obtained from Amyx *et al.* (1960) and Gomes *et al.* (1996) and is presented in Fig. 8. The pore throat size distribution (Amyx *et al.*, 1960; Gomes *et al.*, 1996) is presented in Fig. 9.

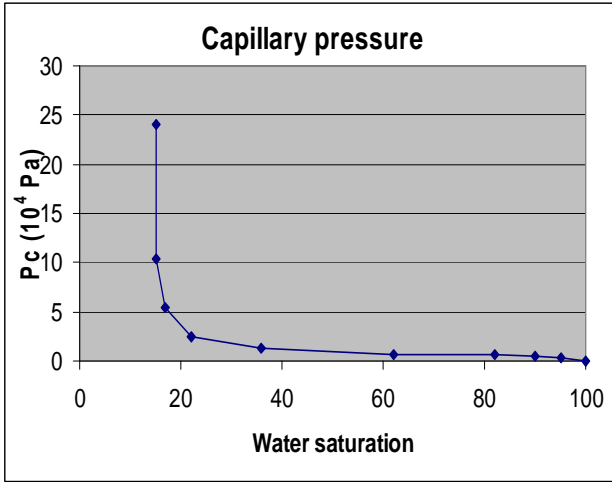


Figure 8. Capillary pressure for Botucatu formation

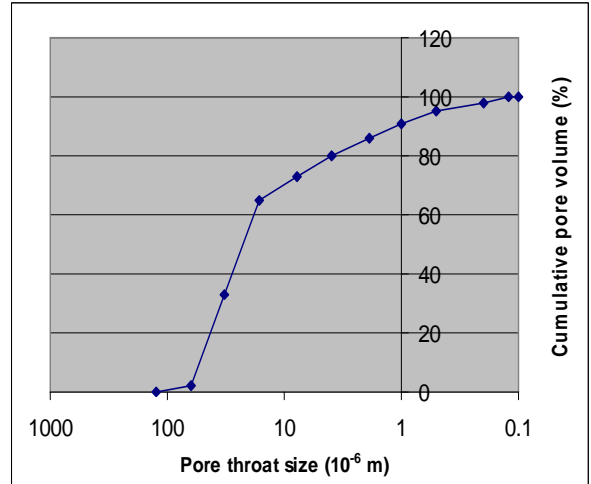


Figure 9. Pore throat sizes for Botucatu rock

2.3. Water Saturation

The plate was water saturated under vacuum, allowing for the determination of the porosity distribution, which is shown in Fig. 10. By using the correlation, shown in Eq. (2), between the measured porosity and the permeability of the samples adjacent to the plate, it is possible to plot a three-dimensional map of the plate absolute permeability, which is presented in Fig. 11.

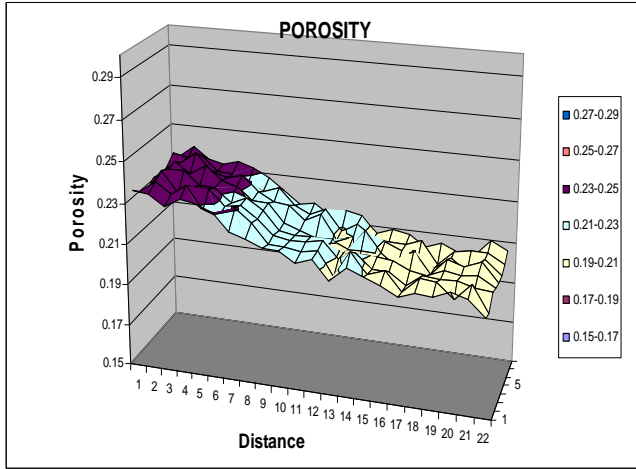


Figure 10. Porosity distribution in rock plate

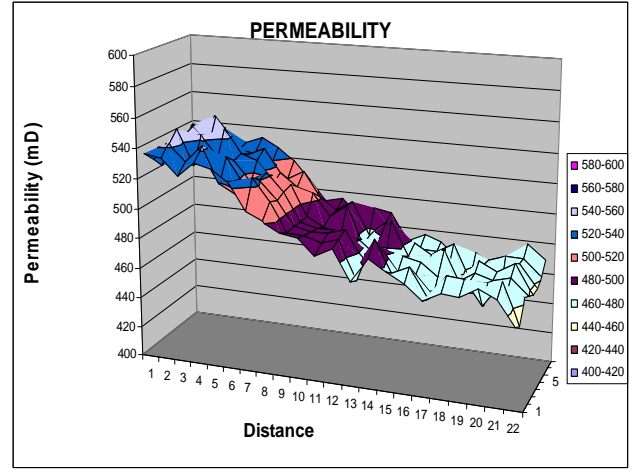


Figure 11. Absolute permeability distribution in rock plate

$$K(mD) = 2173.5 \times (\text{porosity}) + 22.549 \quad (2)$$

where K is the absolute permeability.

2.4. Well Characterization

The wells were characterized by measuring the flow along each one; rate and pressure drop readings were performed, and Poiseuille law was applied; the equivalent radii were found to be $7.18 \times 10^{-4} \text{ m}$ for the right well, and $7.04 \times 10^{-4} \text{ m}$ for the left well.

2.5. Fluid Characterization

The fluids used in the experiment were water and oil; the oil was a viscous transformer mineral oil with a kinematic viscosity of 212cP and density of 750kg/m³; the oil/water interface tension is 4N/m², measured by a DuNouy tensiometer.

A tracer test was performed to observe the flow inside the porous plate; the porous media was saturated with a 10,000ppm solution of NaCl, which was subsequently displaced by a 65,000ppm solution of NaI. The flow inside the plate was observed with the assistance of an X-ray monitoring system. The effluent concentration was monitored by a resistivity measuring system that permitted the calculation of the ion concentration at the outlet, as shown in Fig. 12.

The behavior observed in Fig. 12 was compared to the profile obtained by an analytical calculation; initially, the Peclet number was obtained from the experimental measurement in the position for concentrations 0.1 and 0.9 with Eq. (3).

$$\Delta x_D = x_{D-Cd=0.1} - x_{D-Cd=0.9} = 3.625 \sqrt{\frac{t_D}{N_{pe}}} \quad (3)$$

where x_D is the dimensionless distance, C_D is the tracer concentration, t_D is the dimensionless time and N_{pe} is the Peclet number. A value of $N_{pe} = 15$ was calculated; the longitudinal dispersion coefficient is given by Eq. (4).

$$K_l = \frac{u.L}{\phi.N_{pe}} \approx 4.5 \times 10^{-7} \frac{m^2}{s} = 2.7 \times 10^{-5} \frac{m^2}{min} \quad (4)$$

where K_l is the longitudinal dispersion coefficient, u is the velocity, L is the length of the porous media and ϕ is the porosity.

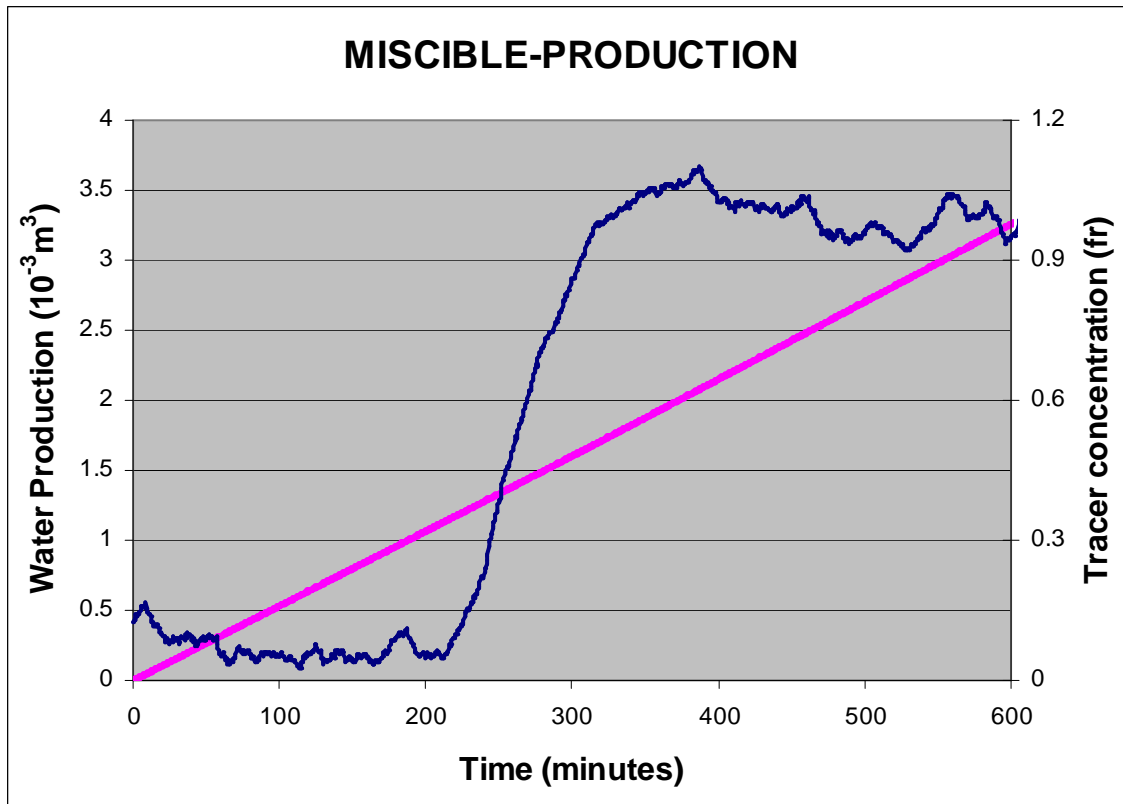


Figure 12. Water and tracer concentration production

The analytical tracer concentration, which is shown in Fig. 13, was calculated by Eq. (5) (Marle, 1981); the dimensionless distance and time used in Eq. (5) are expressed by Eq. (6).

$$C_D = \frac{1}{2} \operatorname{erfc} \left(\frac{x_D - t_D}{2 \sqrt{\frac{t_D}{N_{pe}}}} \right) + \frac{e^{x_D} \cdot N_{pe}}{2} \operatorname{erfc} \left(\frac{x_D + t_D}{2 \sqrt{\frac{t_D}{N_{pe}}}} \right) \quad (5)$$

$$x_D = \frac{x}{L} \dots \dots \dots t_D = \int_0^t \frac{q dt}{V_p} \quad (6)$$

where x is the linear distance, q is the injection rate, t is the time and V_p is the pore volume.

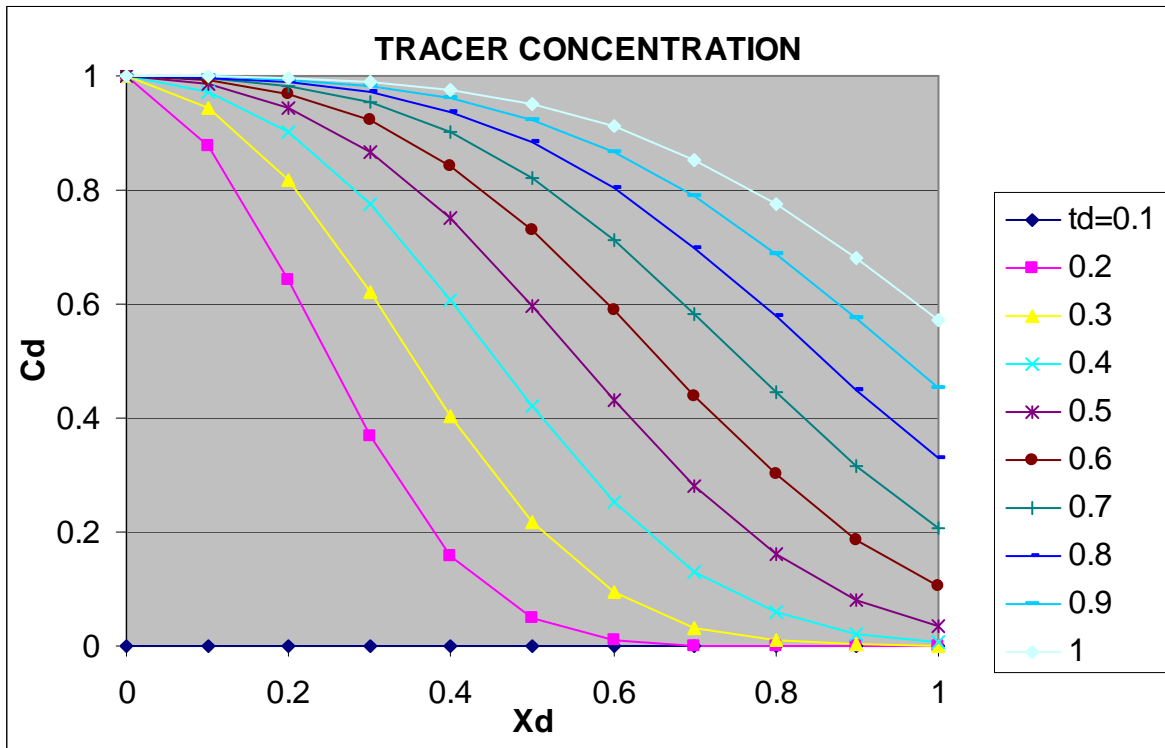


Figure 13. Tracer concentration in dimensionless distance and time

The tracer distribution was further calculated with a commercial numerical simulator, using the data from the experimental test. The main properties are: dimensions, porosity and permeability distribution, longitudinal dispersion coefficient, injection rate. The grid was 88x32x3 blocks and the injection/production simulated consisted of a linear flow with uniform injection, as was observed in the experimental test.

Different X-ray scanned profiles are shown in Figures 14, 16 and 18; the corresponding numerical simulation tracer distribution in the middle layer is presented in Figures 15, 17 and 19, for time = 90 minutes, 162 minutes and 234 minutes, corresponding respectively to dimensionless times of 0.147, 0.396 and 0.572.

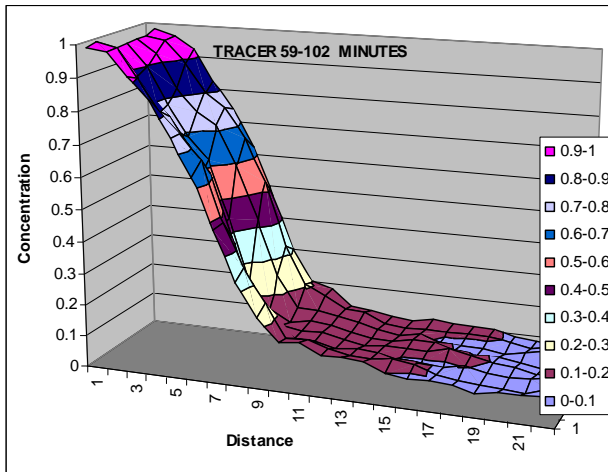


Figure 14. Experimental tracer concentration at 59-102 minutes

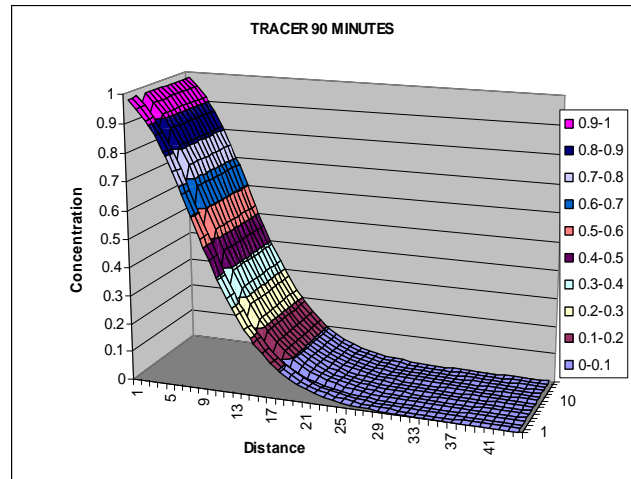


Figure 15. Numerical tracer concentration at 90 minutes

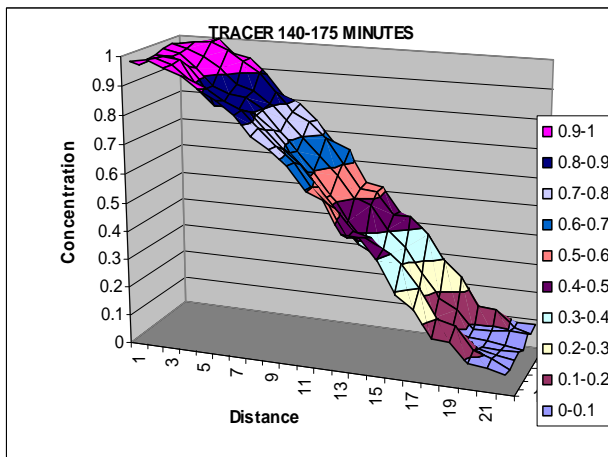


Figure 16. Experimental tracer concentration at time 140-175 minutes

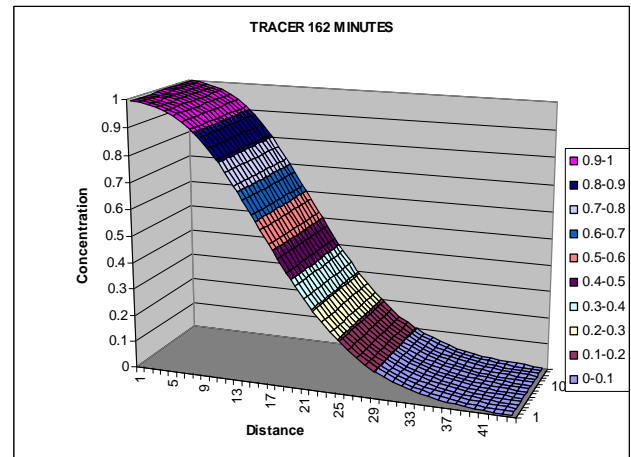


Figure 17. Numerical tracer concentration at 162 minutes

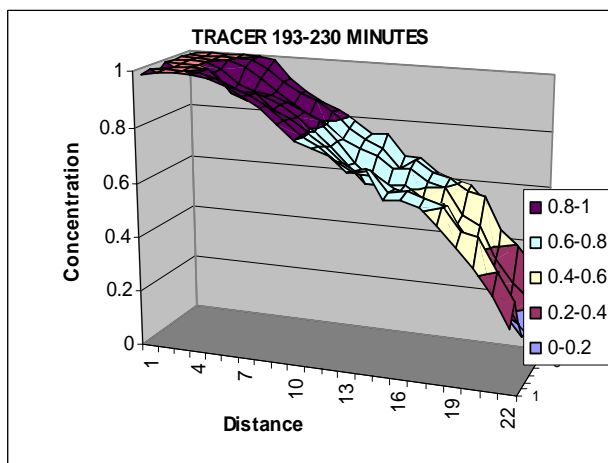


Figure 18. Experimental tracer concentration at time 193-230 minutes

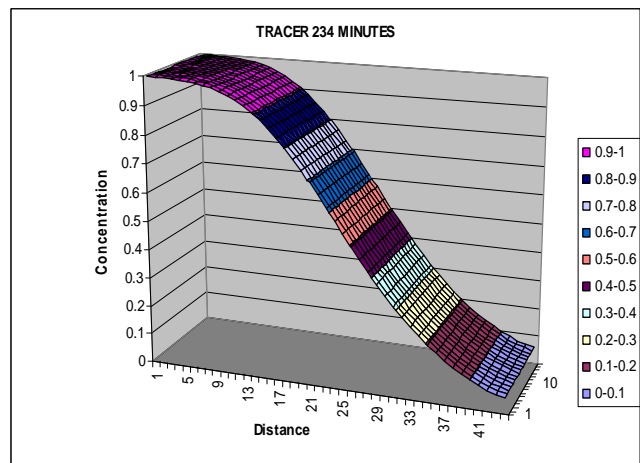


Figure 19. Numerical tracer concentration at 234 minutes

3. Concluding remarks

An adequate rock plate was prepared and used for a displacement test of viscous oil; this plate presented petrographic, petrophysical and flow properties equivalent to those of oil reservoir rocks. The porous media characterization showed a very homogeneous rock regarding the porosity and permeability values, with small variation in properties and a good correlation between them.

The relative permeability curves obtained for the same formation show a strongly water wet rock with adequate oil water relative permeability values. This was confirmed by the capillary pressure curve.

The horizontal wells were characterized. Since they are tied with the absolute permeability in the production/injection along the well, it is very difficult to scale this model to a prototype with real field properties.

A tracer test was performed and showed an appropriate flow performance to study oil displacement with water. The longitudinal tracer test permitted one to calculate the typical Peclet number for the system, which was then used for the analytical calculation of the tracer concentration. Three different times were compared for the experimental, analytical and numerical results of this tracer test. The results are equivalent, although it was not possible to set a fixed time for the experimental test due to the nature of the X-ray scanning process, which took about 40 minutes.

Since the transformation from laboratory scale to field dimensions poses many problems, a decision was made to try to reproduce the behavior observed in the experiment using numerical simulation (and an analytical correlation) still in laboratory units. This was accomplished successfully and constituted an important step in the development of a field scale simulation model, which is the next stage of this project.

4. Acknowledgements

The authors are grateful to the Conselho Nacional de Desenvolvimento Científico e Tecnológico (CTPETRO/CNPq), to FINEP and to PETROBRAS for their financial support to this project. The authors are also grateful to Luiz B. Pompeo Netto and to Leandro A. Fernandes for their great assistance with the experiments.

5. References

- Amyx, J.W., Bass Jr., D.M. and Whiting, R.L., 1960, "Petroleum Reservoir Engineering Physical Properties", McGraw-Hill Book Company, New York, USA. 610 p.
- Chuoque, R.L., Van Meurs, P. and Van Der Poel, C., 1959, "The instability of Slow, Immiscible, Viscous Liquid-Liquid Displacements in Permeable Media", Society of Petroleum Engineers - Transactions AIME, Vol. 216, pp. 188-194.
- Gomes, J.A.T., 1997, "Visualização e Análise do Deslocamento Imiscível e Instável em Meio Poroso Consolidado", PhD Thesis, UNICAMP, 2v.
- Gomes, J.A.T., Tibana, P. and Corrêa, A.C., 1996, "Caracterização Petrofísica e Petrográfica dos Arenitos Berea e Botucatu", Conexpo Arpel, Rio de Janeiro.
- Honarpour, M., Koederitz, L. and Harvey, A.H., 2000, "Relative Permeability of Petroleum Reservoirs". CRC Press Inc., Boca Raton, USA. 143 p.
- Johnson, E.F., Bossler, D.P. and Naumann, V.O., 1959, "Calculation of Relative Permeability from Displacement Experiments", Society of Petroleum Engineers - Transactions AIME, Vol. 216, pp. 370-372.
- Jones, S.C. and Roszelle, W.O., 1978, "Graphical Techniques for Determining Relative Permeability from Displacement Experiments", Journal of Petroleum Technology, pp. 807-817. SPE 6045.
- Marle, C.M., 1981, "Multiphase Flow in Porous Media", Gulf Publishing, Houston, USA, 257p.
- Santos, R.L.A., Bedrikovetsky, P. and Holleben, C.R., 1997, "Optimal Design and Planning for Laboratory Corefloods". Proceedings of the 50th Latin American and Caribbean Petroleum Engineering Conference, Rio de Janeiro, Brazil, pp. 1-11. SPE 39038.

6. Responsibility notice

The authors are the only responsible for the printed material included in this paper.